Surface effects of polyelectrolyte multilayer films on bioactive glass scaffolds

Surface effects of Polyelectrolyte Multilayer Films on bioactive glass scaffolds

Gabriela Imbir[1,2], Francesco Baino[3], Marta Miola[3], Aldona Mzyk[4], Mateusz M. Marzec[5], Enrica Verné[3]

[1]Institute of Metallurgy and Materials Science, Polish Academy of Sciences, Reymonta 25, 30-059 Krakow, Poland,

[2]Institute of Nuclear Physics Polish Academy of Sciences, Radzikowskiego 152, 31-342, Krakow, Poland,

[3]Applied Science and Technology Department (DISAT), Politecnico di Torino, 10129 Turin, Italy,

[4]Department of Health Technology, Danish Technical University, Ørsteds Plads, Kongens Lyngby, DK-2800, Denmark

[5]Academic Centre for Materials and Nanotechnology (ACMiN), AGH University of Science and Technology, al. Mickiewicza 30, 30-059 Krakow, Poland

Abstract:

Bioactive glasses are crucial in regenerative medicine, meeting the demand for biomaterials integrating with bone tissue. This study explores the effect of polymer-based films on bioactive glass, evaluating their impact on biological and physicochemical properties to potentially improve cell-material interaction. Polysaccharide-based films were used to modify a silica-based bioactive glass, analyzing surface features, composition, and bioactivity upon immersion in simulated body fluid. Surface morphology and chemistry analysis confirmed successful functionalization, but no notable differences were found in bioactivity between unmodified and polymer-coated materials. Therefore, the presence of the polymer coating is not detrimental for the apatite-forming ability of the scaffold, while being expected to be beneficial for bone cell attachment, which will deserve future investigation.

Keywords: bioactive glass, polymer-based coatings, polyelectrolytes, ceramic composites, bioactivity

1. Introduction

Bone reconstruction is crucial in biomedical engineering due to rising traumas, bone diseases, or aging and necessitates alternative approaches to stimulate bone healing effectively [1]. Although numerous bone replacement methods utilizing various

biomaterials have been developed, finding an optimal strategy still remains challenging. Bioactive glasses are recognized for their compositional versatility, appealing processability, and ability to promote bone cell growth [1]. Surface properties, including roughness, surface energy and porosity, significantly influence protein absorption, consequently affecting osteoconductivity [2]. However, bioactive glasses face challenges related to poor mechanical strength, irregular porosity, or unwanted degradation rate [2]. Bioactivity is also significant in adapting the structure as a carrier for growth factors [3]. Structural enhancement is thus essential to improve the mechanical strength and refine scaffold physicochemical features; in this regard, the deposition of a polymeric coating on the surface of bioactive glass scaffolds was proved to be a valuable strategy to enhance fracture toughness [4].

Utilizing natural polymer coatings for surface modification of biomaterials is gaining attention to avoid toxicity in the final product [5]. In a previous work, we observed that polyelectrolyte multilayer films (PEM), namely Chitosan (Chi) and Chondroitin Sulfate (CS), are highly suitable for surface functionalization [6]. Owing to their physicochemical properties and simple assembling, these polymers show promise for improving the bioactive glass features. Thus, the present work aims at demonstrating the feasibility of depositing Chi/CS PEMs on the surface of a six-oxide silicate glass scaffold, proposed as a novel biomaterial for bone regeneration, and examining the physicochemical changes on the scaffold surface and the coating effect on *in vitro* bioactivity.

2. Materials and Methods

The synthesis of bioactive silicate glass (BSG; 47.5SiO_2-20CaO-10MgO-2.5P_2O_5-10K_2O-10Na_2O mol.%) followed a previous publication [7]. For making scaffolds by the foam replica method, the melt-derived glass powder was mixed with distilled water and poly(vinyl alcohol) (PVA) in a 30:64:6 (wt.%) ratio. PVA was dissolved in distilled water under vigorous stirring at 60°C for 1 hour until reaching a transparent solution. Due to evaporation, some water was re-added to maintain original ratios. Afterward, glass powder was added and mixed for 10 minutes to ensure uniform dispersion. Polyurethane sponge blocks (side 5 mm) were soaked in the suspension as templates for scaffold production. Thermal treatment in furnace at 700°C for 3 hours allowed polyurethane burn-off and glass particle sintering.

2.1.BSG scaffolds functionalized by PEM

Sintered scaffolds were modified using three bilayers of Chi (MW: ~250 kDa) and CS (MW: ~25 kDa), denoted as (Chi/CS)3, through the Layer-by-Layer (LbL) deposition via dip coating. The scaffolds were first treated with 5 M NaOH for 20 minutes to activate their surface with a negative charge, promoting electrostatic interactions with the polyelectrolytes. Chi and CS were prepared in 0.15 M NaCl at 0.5 mg/mL concentration, with Chi initially dissolved in 0.1 M acetic acid due to its poor water solubility. To enhance electrostatic interactions, the pH of both solutions was adjusted to 5.5. Scheme of final material is illustrated in Fig.1.

2.2. Surface chemistry and morphology

Surface morphology was examined through Field-Emission Scanning Electron Microscopy (FESEM, SupraTM 40, Zeiss) with energy-dispersive X-ray spectroscopy, at an acceleration voltage of 5-10 kV and beam current of 4.0 nA. A Pt thin film was sputtered on the non-conductive samples to facilitate imaging.

X-ray Photoelectron Spectroscopy (XPS) measurements were performed by a PHI VersaProbeII Scanning XPS system, using monochromatic Al Kα X-rays (1486.6 eV) focused on a 100 µm spot across a 400 µm × 400 µm area.

2.3. In vitro bioactivity tests

Uncoated and PEM-coated scaffolds underwent bioactivity tests by soaking in simulated body fluid (SBF), following Kokubo's protocol [8] to verify a possible influence of PEM coating on bioactivity. Samples were incubated in SBF for 48 hours and 7 days at 37°C under static conditions, with the solution refreshed every 48 hours to mimic fluid circulation, and the pH was monitored daily. The mass-to-volume ratio for uncoated and coated type was 1.5 mg/mL. Samples were investigated using FESEM/EDS.

3. Results and discussion

3.1.Surface morphology

BSG scaffold, as such (Fig. 1B), exhibited a characteristic network of porous, spongy structure, as previously reported [7]. After (Chi/CS)3 functionalization, honeycomb-like submicropores emerge, but the whole structure retained a resemblance to trabecular bone architecture (Fig.1C) [9]. High viscosity of chitosan, caused by intermolecular and intramolecular hydrogen bonding, affected the pore structure and pre-treatment using acetic acid could alter the structure degradation by formation of equiaxial pores [10].

Employing the LbL and maintaining a pH below the pK_a of Chi lead to the presence of ionized amino groups, which facilitates strong interaction with sulfonic groups of CS [11]. A formed hydrogen bonding, attributed to LbL, induces a microporous morphology after immersion in a basic solution [12]. However, acidic environment can also initiate micropores formation. For example, low pH of PAH/PAA film caused the cleavage of ionic bonds through the protonation of carboxylate groups of PAA [13]. Polymer chains self-arrange when the pHs of polymer solutions are near or higher than the pK_a of Chi

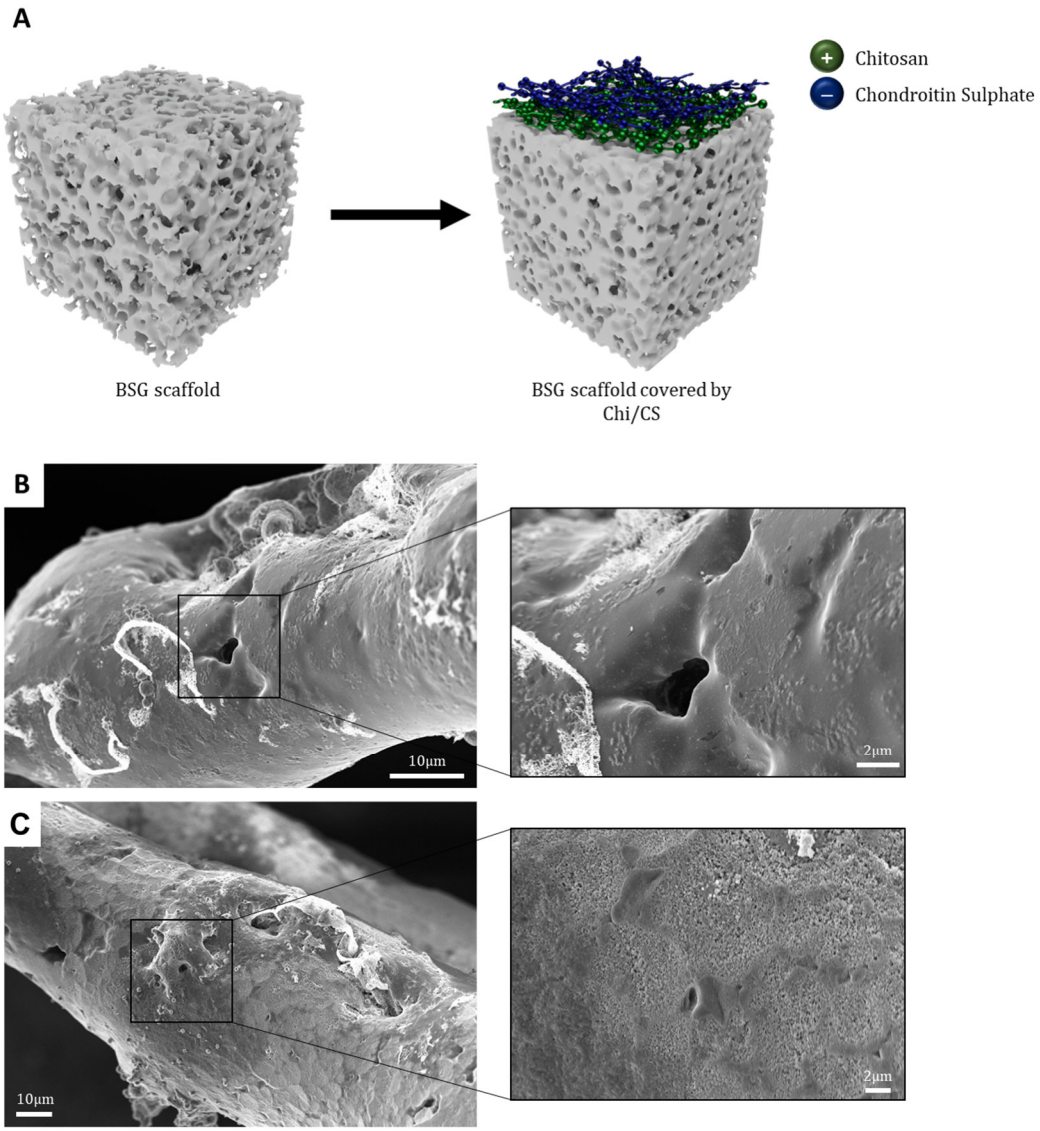

Fig. 1 *A) Scheme of PEM coated-BSG scaffold deposited via dip coating, with surface topography of a BSG scaffold B) as such, and C) coated by (Chi/CS)3*

[11]. In this case, functional surface group reorganization on the coating, caused by layer interpenetration, can result in micropore formation.

XPS further investigated the surface chemistry and functional group ratios after modifications, focusing on carbon, nitrogen, oxygen, and sodium elements (Fig. 2, Tab.1).

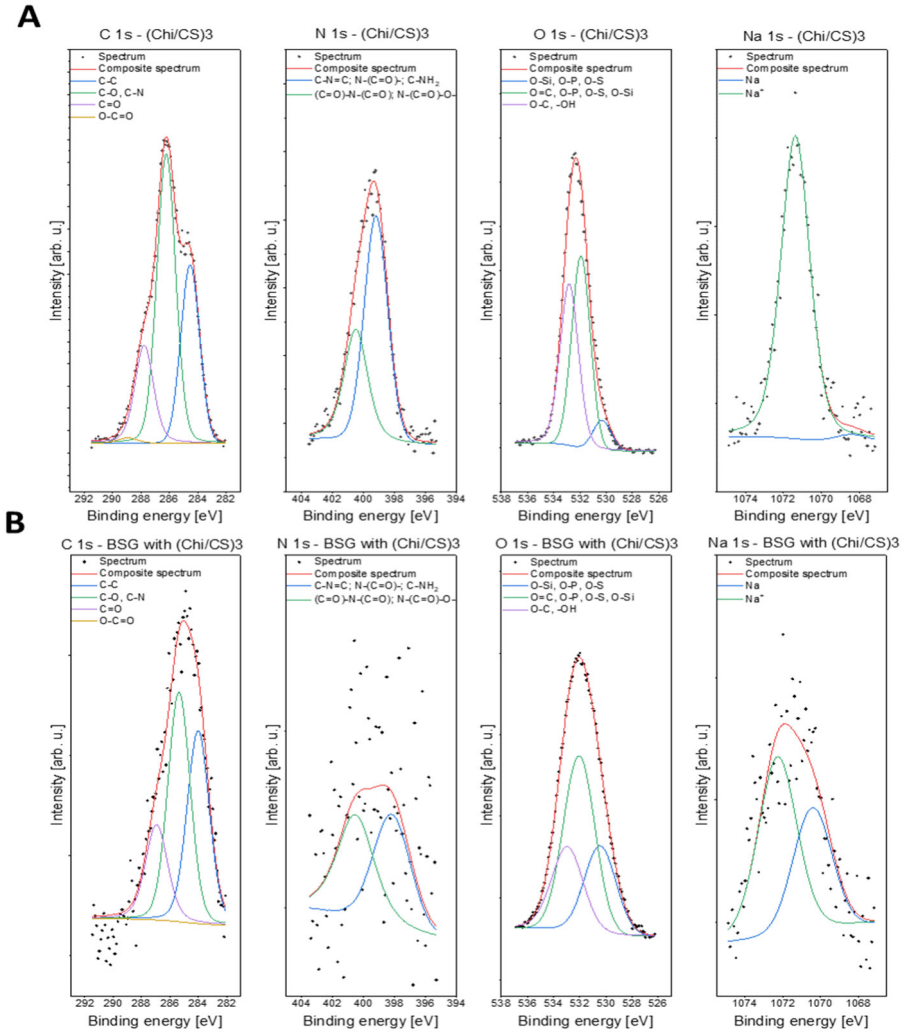

Fig. 2 *High resolution XPS measurement for A) (Chi/CS)3 film and B) BSG with (Chi/CS)3.*

The polymer coating altered the scaffold's surface chemistry, as indicated by the increase of P, S, and C atomic percentages. The change was specifically noticed in the level of –COOH group. The coating spectrum displayed four peaks for C 1s: first, at 284.8 eV associated with the C-C type carbon bonds, a second, at 285.9 eV, due to C-O or C-N bonds, a third, at 287.0 eV from C=O groups and a fourth, at 288.0 eV related to O-C=O bonds [14]. Two peaks were detected for N 1s, the first point at amine or amide groups, and the second indicates (C=O)-N-(C=O) and/or N-(C=O)-O- type compounds [14,15]. The O 1s region showed three peaks at 530.1, 532.3, and 533.6 eV, attributed to inorganic oxygen-containing species, C=O and/or Si-O and/or O-P and/or O-Si bonds, and C-O and/or -OH bonds, respectively [15]. Additionally, the peak originating from Na 1s

demonstrated two lines: the first, centered at 1068.7 eV, may suggest a crystal like state of sodium and the second line at 1071.3 eV indicates the Na^+ [15]. The observed peaks could be attributed to sample immersion in 0.15 M NaCl.

Table 1 *Surface analysis (atomic %) of coated and uncoated BSG scaffolds*

	C				**N**		**O**			**Na**	
Binding energy [eV]	284.8	285.9	287.0	289.0	399.2	400.7	530.1	532.2	533.6	1068.7	1071.3
Functional group	C-C	C-O C-N	C=O	O-C=O	C-NH C-N=C	(C=O)-N N-C=O	O-Si O-P O-S	O=C O-Si O-P	O-C -OH	Na	Na^+
(Chi/CS)3	15.1	25.2	9.7	1.3	5.3	3.4	3.4	17.3	15.9	0.8	2.6
BSG with (Chi/CS)3	7.0	7.7	4.8	2.4	3.0	3.0	17.0	31.3	17.2	3.0	3.4

Chi/CS exhibits either electrostatic interactions or hydrogen bonding between Si-OH groups from the glass, and C=O, NH from chitosan [5]. Whereas, CS demonstrate sulfate and carboxylic groups [6]. We noted an increased contribution of carboxylic groups in polymer-coated BSG rather than S-O, suggesting different coordination of chitosan atoms or the replacement of sulfate groups with the OH groups of scaffold [16].

The *in vitro* bioactivity test aimed to explore the impact of surface functionalization on hydroxyapatite development. According to the mechanism of hydroxyapatite-like layer formation, the exchange of H^+ ions between the SBF solution and the BSG triggers the release of Na^+, Ca^{2+}, and Mg^{2+}. Upon interaction with phosphate ions, the layer transforms into an amorphous calcium phosphate layer with a low Ca/P ratio, which eventually crystalizes into bone-like apatite, with an ideal stoichiometric ratio of 1.67 [17].

SEM images (Figure 3 A – D) reveled the progress of HA formation. Following 48 h of immersion, struts and walls of polymer-free scaffold demonstrated small globular-like CaP nuclei with a Ca/P molar ratio of 1.20, below the stoichiometric range. After 7 days, the scaffolds appeared with higher quantity of globular-like structures, and the Ca/P ratio increased to 1.7, slightly above the ideal value.

The (Chi/CS)3 coated scaffold revealed small-scale nuclei after 48 h, with a high Ca/P ratio of 1.91, transitioning to more uniform globular HA structure during 7 days. However, the coated Ca/P ratio decreased to 1.41, suggesting the formation of a Ca-deficient hydroxyapatite thin film, regularly found on the surface of BSG soaked in SBF [18]. The PEM coating potentially influences on apatite-forming ability through

carboxylic groups, which enhance calcium phosphate layer development by attracting Ca^{2+} ions on polyelectrolyte surface. Over time, this process contributes to denser structure of calcium phosphate layer [19]. The presence of –COOH groups can also promote the adhesion of bone cells, as reported in literature[20].

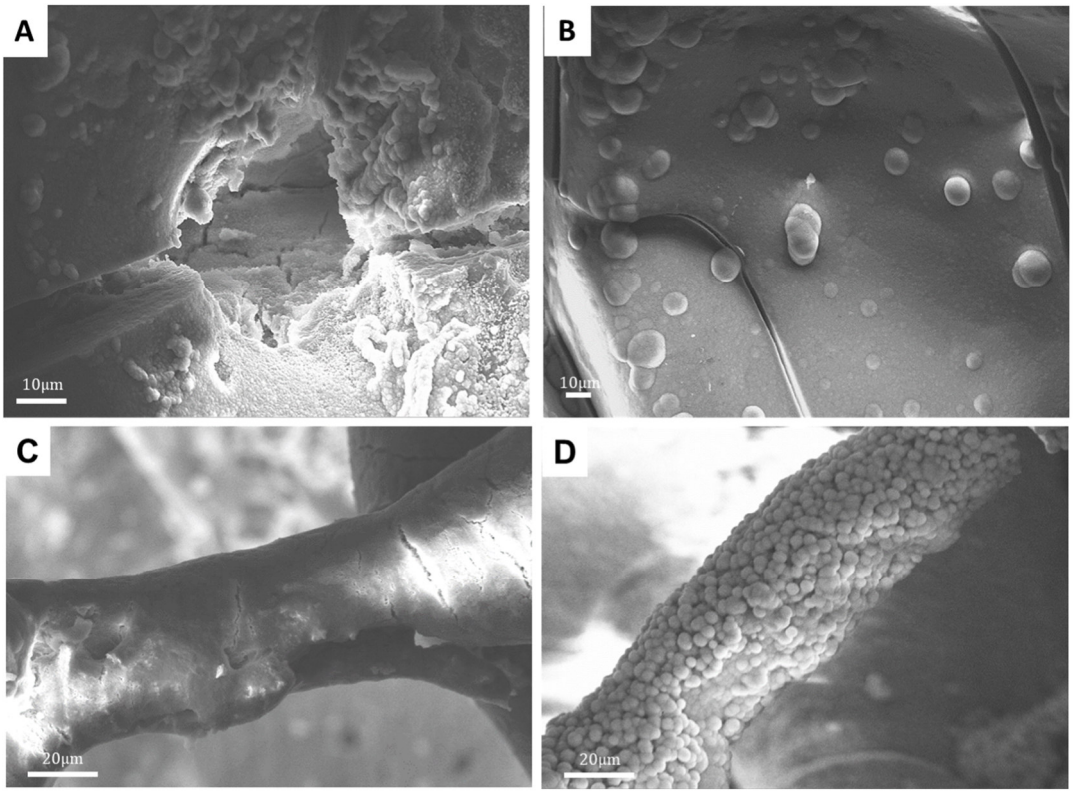

Fig. 3 *SEM micrographs of uncoated and coated BSG scaffold after 48 h (A,C) and seven days (B,D), respectively.*

4. Conclusions

The presented study provided valuable insights on PEM-coated BSG scaffolds, exploring their physicochemical attributes for biomedical applications. Advanced analysis confirmed the presence of film upon the BSG scaffold and highlighted the influence of film's carboxylic group on scaffold bioactivity. Further research is essential to investigate the impact of functional groups, employing additional measurement techniques and experiments to evaluate biomedical potential.

Acknowledgements:

PEM coatings were manufactured within a project financed by the National Centre of Science in Poland, grant No. 2014/15/N/ST8/02601. Characterization was supported by The European Virtual Institute on Knowledge-based Multifunctional Materials AISBL (KMM-VIN) Research Fellowship, call 2020 (grant to Gabriela Imbir).

References:

[1] Q. Fu, E.Saiz, M.N. Rahaman, A.P.Tomsia, Mater Sci Eng C Mater Biol Appl. 31(7) (2011) 1245–1256.

[2] B. Lowe, M.P. Ottensmeyer, C. Xu, Y. He, Q. Ye, M.J. Troulis, , J. Funct. Biomater. 10 (2019) 1–18.

[3] Q. Yao, P. Nooeaid, R. Detsch, J.A. Roether, Y. Dong, O.M. Goudouri, D.W. Schubert, A.R. Boccaccini, J. Biomed. Mater. Res. - Part A. 102 (2014) 4510–4518.

[4] Q. Fu, W. Jia, G. Y. Lau, A. P. Tomsia, J. Biomed. Mater. Res. - Part B. 106 (2018) 925-1413

[5] A. Motealleh, S. Eqtesadi, A. Pajares, P. Miranda, J. Mech. Behav. Biomed. Mater. 84 (2018) 35–45.

[6] G. Imbir, K. Trembecka-Wójciga, P. Ozga, R. Schirhagl, A. Mzyk, Col.Surf. B Bioint. 225 (2023) 113269.

[7] F. Baino, E. Fiume, Mater. Lett. 245 (2019) 14–17.

[8] T. Kokubo, H. Takadama, Biomat. 27 (2006) 2907–2915.

[9] V. Karageorgiou, D. Kaplan, Biomat. 26 (2005) 5474–5491.

[10] S.J. Florczyk, D.J. Kim, D.L. Wood, M. Zhang, J. Biomed. Mater. Res. - Part A. 98 (2011) 614–620.

[11] W. Sui, L. Huang, J. Wang, Q. Bo, Col. Surf. B Bioint. 65 (2008) 69–73.

[12] S. Bai, Z. Wang, J. Gao, X. Zhang, Eur. Polym. J. 42 (2006) 900–907.

[13] B.Y. Kim, M.L. Bruening, Langmuir. 19 (2003) 94–99.

[14] M.J. Genet, C.C. Dupont-Gillain, P.G. Rouxhet, Med. Appl. Col. (2008).

[15] A.V. Naumkin, A. Kraut-Vass, C.J. Powell, NIST Stand. Ref. Database 20, Natl. Inst. Stand. Technol. Gaithersbg. (2000).

[16] R.M. Lauder, Complement. Ther. Med. 17 (2009) 56–62.

[17] M. Araújo, M. Miola, G. Baldi, J. Perez, E. Verné, Materials. 9 (2016) 226.

[18] L. Pazourková, G. S. Martynková, M. Šupová, Mat.Today: Proc. 52 (2022) 227-231.

[19] A. Salama, M. El-Sakhawy, Carbohydr. Polym. 113 (2014) 500–506.

[20] B. Cao, Y. Peng, X. Liu, J. Ding, ACS Appl.Mat&Inter. 9 (2017) 23265-24392.